

Dinara A. Birimzhanova¹ , Irina S. Irgibaeva^{1*} , Nikolay N. Barashkov² 

¹*L.N. Gumilyov Eurasian National University, Astana, Kazakhshtan;*

²*Micro Tracers, Inc., San Francisco, California, USA*

(*Corresponding author's e-mail: irgsm@mail.ru)

Quantum-Chemical Study of Aggregation of 5-(4'-Dimethylaminobenzylidene)Barbituric Acid

Decreasing fluorescence efficiency in the solid-state is general and is mainly attributed to the intermolecular vibronic interactions, which induce the nonradiative deactivation process. Whereas the isolated dye molecules are virtually non-luminescent in dilute solutions, they become highly emissive upon solution thickening or aggregation in poor solvents or in the solid-state show an increase of luminescence intensity, the phenomenon of the aggregation-induced emission (AIE phenomenon). The development of efficient luminescent materials is a topic of great current interest. Theoretical calculation shows that the dye molecules' aggregation-induced emission characteristics result from intermolecular interactions. Utilizing such features, the molecules can be employed as fluorescent probes for the detection of the ethanol content in aqueous solutions. Quantum-chemical calculations using the method of density functional theory the computations of structure and electronic spectra of aggregated forms of 5-(4'-dimethylaminobenzylidene)barbituric acid and the Gaussian 98 program packages have been performed. The unusual spectral behavior of 5-(4'-dimethylaminobenzylidene)barbituric acid was investigated theoretically by the DFT method and its time-dependent variant TDDFT. Carried out calculations using Zindo, as well as *ab initio* calculations, confirm the appearance of a new band during aggregation and its shift to the red region when the number of molecules increases.

Keywords: barbituric acid, electronic spectra, dye molecules, aggregation-induced emission, theoretical study, hydrogen bond, electronic states, valence vibrations.

Introduction

Currently, fluorescent organic nanoparticles (FONs) are less studied than fluorescent inorganic semiconductors or metallic nanoparticles, which have attracted significant research interest due to their unique properties related to quantum effects at the micro level. Due to these properties, organic nanoparticles are intensively studied for use in various fields, including fluorescent biological markers, photovoltaic cells, LEDs and optical sensors. It is expected that fluorescent organic nanoparticles have a higher potential in comparison with their inorganic counterparts, since they are more diverse and there are many methods of their synthesis and preparation of nanoparticles.

One of the many potential applications of FON is related to their ability to show a change in fluorescence depending on the size, while this fluorescence property is very different from the similar characteristic for the molecular form of the organic compound of the same nature. It is well known the fluorescence quantum yield of organic chromophores usually decreases in the solid state, although they have a high fluorescence quantum yield in solution. This decrease in the fluorescence quantum yield in the solid state is usually associated with intermolecular vibrational interactions, which cause nonradiative relaxation processes, such as exciton binding, excimer formation, migration of excitation energy to trapped impurities, etc. However, some exceptions have been reported [1–6], for example, for derivatives of barbituric acid [7–9], which show enhanced emission in the solid state, rather than quenching of the glow.

This work is devoted to the theoretical study of optical electronic and vibrational spectra of 5-(4'-dimethylaminobenzylidene)barbituric acid (DM).

Computational Details

Quantum-chemical calculations of the geometric structure of the DM molecule (Fig. 1) were carried out with the density functional method (DFT) using the Gaussian 98 software package. Geometry optimization was carried out using a three-parametric hybrid Becke method with gradient-correction correlation of the Lee, Yang and Parr functional (B3LYP) and a standard 6-31G(d) basis set. The electronic spectra were ob-

tained taking into account the time dependence of the density functional theory (TDDFT) method, where discrete spectra of energy excitation and corresponding oscillator strengths were estimated for several tens of low-energy singlet transitions [10, 11].

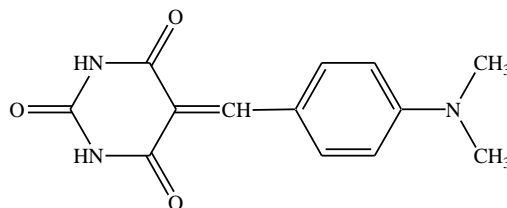


Figure 1 Structural formula of DM

Results and Discussion

Electronic absorption spectra of the DM molecule and its complexes were calculated using wave functions of the ground state. The absorption wavelength for a molecule is 371.58 nm, for aggregations of two, three and four molecules this band shifts to the long-wavelength region and is 379 nm. As mentioned above, the observed absorption band in the long-wavelength region of 460 nm was not found in model calculations of complexes of DM molecules of two, three, and four.

Complex formation occurs due to intermolecular hydrogen bonding. Table 1 shows the frequencies of valence vibrations of DM for an optimized geometric configuration.

Table 1

Frequencies and forms of valence vibrations of bonds of DM

Valence vibrations, cm^{-1}	Forms of vibrations
$\nu(\text{C}_1\text{-O}_7)$ 1841.99	$0.65 d^x(\text{C}_1) + 0.22 d^y(\text{C}_1) - 0.37 d^x(\text{O}_7) - 0.12 d^y(\text{O}_7)$
$\nu(\text{N}_2\text{-H}_8)$ 3615.50	$-0.05 d^x(\text{N}_2) + 0.05 d^y(\text{N}_2) + 0.73 d^x(\text{H}_8) - 0.64 d^y(\text{H}_8)$
$\nu(\text{C}_3\text{-O}_9)$ 1790.45	$0.06 d^x(\text{C}_3) + 0.53 d^y(\text{C}_3) - 0.03 d^x(\text{O}_9) - 0.32 d^y(\text{O}_9)$
$\nu(\text{C}_4\text{-C}_{12})$ 1602.07	$-0.17 d^x(\text{C}_4) - 0.05 d^y(\text{C}_4) + 0.29 d^x(\text{C}_{12}) + 0.05 d^y(\text{C}_{12})$
$\nu(\text{C}_5\text{-O}_{10})$ 1752.57	$-0.33 d^x(\text{C}_5) + 0.46 d^y(\text{C}_5) + 0.21 d^x(\text{O}_{10}) - 0.26 d^y(\text{O}_{10})$
$\nu(\text{N}_6\text{-H}_{11})$ 3612.97	$-0.02 d^x(\text{N}_6) - 0.07 d^y(\text{N}_6) + 0.21 d^x(\text{H}_{11}) + 0.95 d^y(\text{H}_{11})$

Due to structural features, derivatives of barbituric acid can form intermolecular hydrogen bonds. Let's look at dimers as an example (Fig. 2).

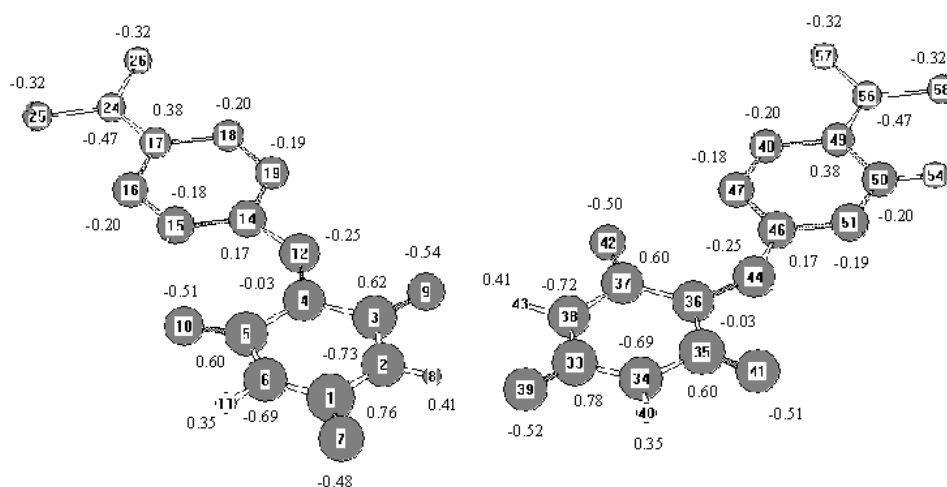


Figure 2. Complex of two molecules — configuration 1

As can be seen in Figure 2, two hydrogen bridges ($\text{N}_2\text{H}_8 \dots \text{O}_{39}$) and ($\text{N}_{38}\text{H}_{43} \dots \text{O}_9$) with lengths of 2.88 Å and 2.89 Å are formed in the dimer, respectively. The calculation of vibrational frequencies (Table 2)

indicates the formation of a hydrogen bond: the valence vibration of N₂-H₈ shifts to the low-frequency region, from 3615.50 cm⁻¹ in the monomer (Table 1) to 3323.90 cm⁻¹ in the dimer. The characteristic vibration of the C₃₃-O₃₉ carbonyl bond varies from 1841.99 cm⁻¹ to 1802.80 cm⁻¹. The same is observed for the second hydrogen bridge.

Table 2

Frequency and form of valence vibration bonds in a complex of two DM molecules

Valence vibrations, cm ⁻¹	Forms of vibrations
ν (C ₁ -O ₇) 1844.87	$-0.08 d^x(C_1) + 0.64 d^y(C_1) + 0.05 d^x(O_7) - 0.36 d^y(O_7)$
ν (N ₂ -H ₈) 3323.90	$-0.05 d^x(N_2) + 0.02 d^y(N_2) + 0.67 d^x(H_8) - 0.28 d^y(H_8)$
ν (C ₃ -O ₉) 1731.72	$0.41 d^x(C_3) + 0.28 d^y(C_3) - 0.23 d^x(O_9) - 0.15 d^y(O_9)$
ν (C ₄ -C ₁₂) 1599.45	$0.03 d^x(C_4) - 0.15 d^y(C_4) - 0.07 d^x(C_{12}) + 0.24 d^y(C_{12})$
ν (C ₅ -O ₁₀) 1774.74	$0.51 d^x(C_5) - 0.12 d^y(C_5) - 0.30 d^x(O_{10}) + 0.07 d^y(O_{10})$
ν (N ₆ -H ₁₁) 3612.30	$-0.06 d^x(N_6) - 0.05 d^y(N_6) + 0.77 d^x(H_{11}) + 0.64 d^y(H_{11})$
ν (C ₃₃ -O ₃₉) 1802.80	$0.48 d^x(C_{33}) + 0.37 d^y(C_{33}) - 0.26 d^x(O_{39}) - 0.19 d^y(O_{39})$
ν (N ₃₄ -H ₄₀) 3613.95	$0.01 d^x(N_{34}) - 0.07 d^y(N_{34}) - 0.08 d^x(H_{40}) + 0.99 d^y(H_{40})$
ν (C ₃₅ -O ₄₁) 1790.78	$0.36 d^x(C_{35}) - 0.21 d^y(C_{35}) - 0.21 d^x(O_{41}) + 0.12 d^y(O_{41})$
ν (C ₃₆ -C ₄₄) 1602.67	$-0.14 d^x(C_{36}) - 0.10 d^y(C_{36}) + 0.20 d^x(C_{44}) + 0.18 d^y(C_{44})$
ν (C ₃₇ -O ₄₂) 1756.02	$-0.15 d^x(C_{37}) + 0.49 d^y(C_{37}) + 0.07 d^x(O_{42}) - 0.30 d^y(O_{42})$
ν (N ₃₈ -H ₄₃) 3352.15	$-0.05 d^x(N_{38}) + 0.02 d^y(N_{38}) + 0.66 d^x(H_{43}) - 0.29 d^y(H_{43})$

Analysis of the vibrational frequencies and forms of normal vibrations of the DM and its dimer shows the mode with the largest contribution from the valence bond NH, which participates in the formation of a hydrogen bond with the C=O group of the neighboring molecule, has the highest amplitude of oscillations during complex formation. At the same time, it was interesting to find out how the formation of hydrogen bonds affects the electronic spectrum of the compound in solution.

As can be seen from Table 3, the absorption band at 371.58 nm, characteristic of a monomolecule, is slightly shifted to the long-wave region (378.49 nm) and at the same time a new absorption band (396.17 nm) appears for the S₁ state with zero oscillator strength.

Table 3

Calculated energies and wavelengths of electronic transitions of two DM molecules

Transition	Energy of transition, eV	Wave function	Wavelength nm	Oscillator strength
S ₁ ($^1\pi \rightarrow \pi^*$)	3.13	$^1\Phi_1 = 0.71 (\varphi_{136} \rightarrow \varphi_{137})$	396.17	0.0
S ₃ ($^1\pi \rightarrow \pi^*$)	3.27	$^1\Phi_1 = 0.40 (\varphi_{135} \rightarrow \varphi_{137}) - 0.39 (\varphi_{136} \rightarrow \varphi_{138})$	378.49	0.0623
S ₄ ($^1\pi \rightarrow \pi^*$)	3.39	$^1\Phi_1 = 0.38 (\varphi_{135} \rightarrow \varphi_{137}) + 0.39 (\varphi_{136} \rightarrow \varphi_{138})$	365.22	0.1248

In the case of a complex of three molecules, two models with different structures are formed — flat (Fig. 3) and non-planar (Fig. 4). The flat configuration of three molecules is more stable by 4.15 kcal/mol.

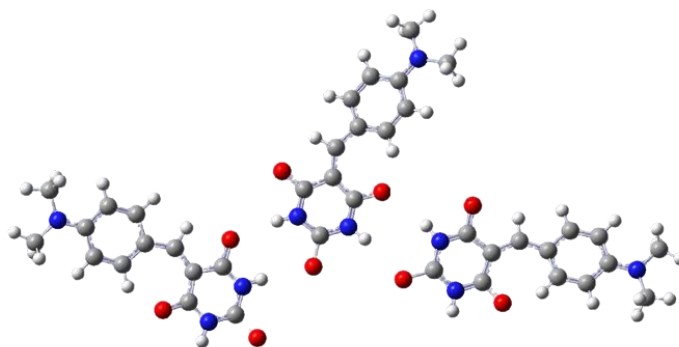


Figure 3. Complex of three molecules with flat structure — configuration 1

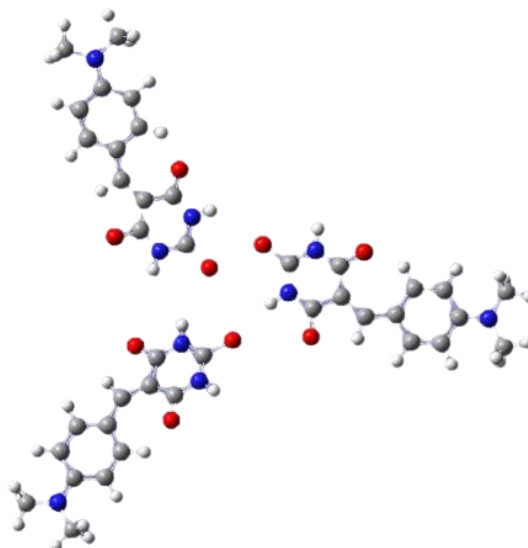


Figure 4. Complex of three molecules with a non-planar structure — configuration 1

Models of two, three and four molecules (Fig. 5) with a configuration different from the above were also calculated.

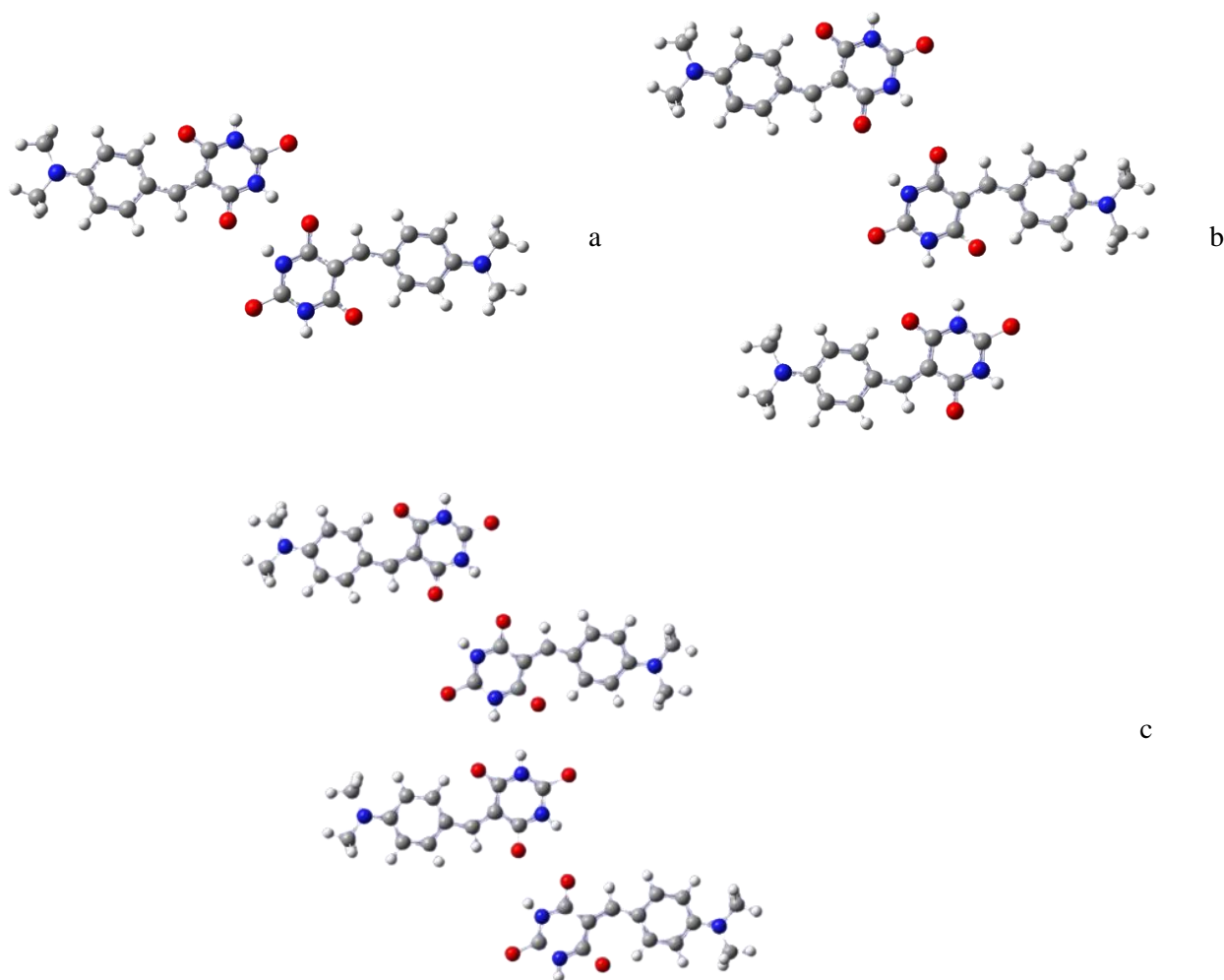
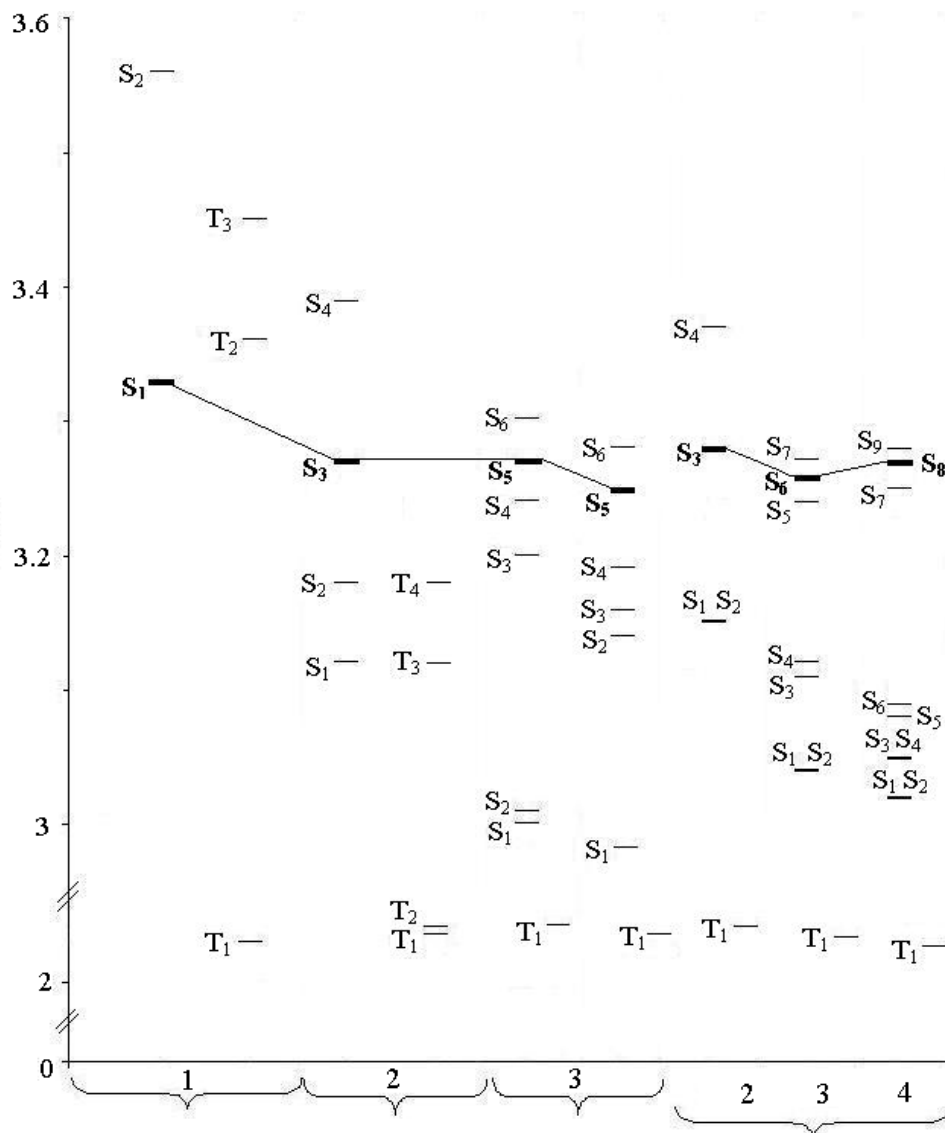


Figure 5. Complex of two (a), three (b) and four molecules (c) — configuration 2

Figure 6 shows the distribution of electronic levels for a monomolecule and complexes of several molecules. The electronic levels corresponding to the absorption band of the monomolecule are selected. When the number of molecules increases, new low-lying electronic levels appear. In both cases, both for configuration 1 and for configuration 2, a new absorption band (absorption band for aggregation), electronic level S_1 , appears. For configuration 1, the oscillator strength for this band is zero, for configuration 2, this band has a weak oscillator strength: for two molecules, the absorption band is 392.55 nm, for three molecules — 407.80 nm, for four molecules — 409.32 nm. Also, when the number of molecules increases, degenerate states appear, for example, for a complex of four molecules $S_1 = S_2 = 3.03$ nm, $S_3 = S_4 = 3.05$ nm.

It follows from the given data that upon aggregation of a large number of molecules DM, the absorption band of the monomolecule shifts to a longer wavelength region and a new band characteristic of aggregation appears.



Axis y — Energy, eV, axis x — electronic levels.

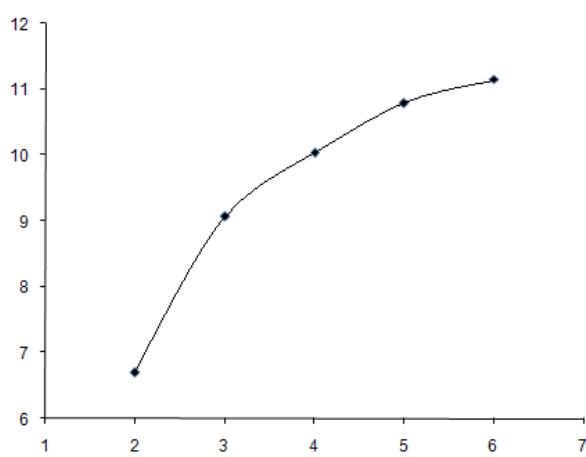
Configuration 1: 1 — monomolecule; 2 — a complex of two molecules; 3 — a complex of three molecules (non-planar and planar structure). Configuration 2: 2, 3, 4 — complexes of two, three and four molecules

Figure 6. Distribution of electronic levels for monomolecules and complexes of two, three and four DM molecules with different configurations

According to calculations, the energy difference between the highest occupied and the lowest unoccupied molecular orbitals, the gap between HOMO and LUMO decreases with an increase in the number of molecules, this is observed both for configuration 1 and configuration 2.

It has also been suggested that an intermolecular proton transfer reaction from a nitrogen atom to an oxygen atom may occur during aggregation. Two-proton transfer for a monomolecule, complexes of two, three and four molecules with different configurations was calculated. However, according to the distribution of electronic levels for a complex of three molecules, two-proton transfer does not occur. There is only stabilization in the excited state, that is, a decrease in the energy barrier for two-proton transfer. Energy difference in the ground state is 1.05 eV for configuration 1 and configuration 2, energy difference in the excited state for levels S_6 , S_5 , S_4 is 0.99 eV for both configurations. States S_6 , S_5 , S_4 correspond to the absorption wavelength of the monomolecule (371 nm). The S_1 states correspond to a new absorption band shifted to the long-wavelength region (for aggregation). For configuration 1, the oscillator strength for the S_1 state is zero. For configuration 2, the oscillator strength for the first excited state is 0.0004 (NH) and 0.0011 (2OH).

Figure 7 shows a hydrogen bond diagram for a dimer, a complex of three, four, five, and six molecules. As can be seen, with an increase in the number of molecules, the energy of hydrogen bond increases. It is assumed that with a further increase in the number of aggregating DM molecules, this tendency is preserved.



Axis y — hydrogen bond energy, eV, axis x — number of molecules

Figure 7. Diagram of changes in the energy of the hydrogen bond between DM molecules

When the number of aggregating molecules increases, this band shifts to a longer wavelength region. For a complex of two molecules, this band is 392 nm, for three — 408 nm, for four molecules — 409 nm, and for a complex of five molecules, the band with charge transfer is 411 nm.

Sandwich complexes of two, four, six, eight and ten molecules were also calculated using the Zindo method (Fig. 8, Table 4).

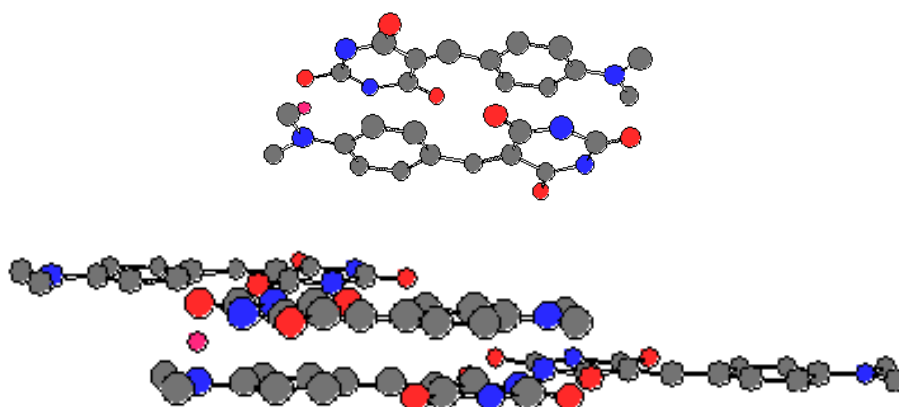


Figure 8. Sandwich complexes of two and four molecules DM

**Energy and wavelengths of electronic transitions calculated by the Zindo method
for molecular DM sandwich complexes**

2 molecules				4 molecules			
R (N-O), Å	E, eV	λ , nm	f	R (N-O), Å	E, eV	λ , nm	f
2.4	2.10	591	0.3485	2.4	2.17	572	0.4320
	3.51	353	0.1107		3.53	351	1.1046
	3.84	323	0.2026		3.82	324	0.6658
2.5	2.42	513	0.4722	2.5	2.48	500	0.5498
	3.50	354	0.2054		3.50	354	1.3224
	3.86	321	0.1089		3.83	323	0.3824
6 molecules				8 molecules			
R (N-O), Å	E, eV	λ , nm	f	R (N-O), Å	E, eV	λ , nm	f
2.4	2.19	567	0.4293	2.4	2.23	556	0.5073
	3.55	349	0.9919		3.56	348	0.5275
	3.86	321	0.8270		3.83	323	1.0770
2.5	2.50	496	0.5686	2.5	2.52	491	0.6202
	3.54	350	1.4535		3.55	349	1.4867
	3.86	321	0.3540		3.88	319	1.1954
10 molecules							
R (N-O), Å	E, eV	λ , nm	f				
2.4	2.28	543	0.5653				
	3.45	360	0.5595				
	3.85	321	0.5798				
2.5	2.58	480	0.6573				
	3.48	356	0.8648				
	3.87	320	1.9797				

Note. R (N-O) — distance between molecules in the upper and lower planes.

Table 4 shows three absorption bands. Two bands in the region of about 350 and 320 nm, don't change with increasing molecules. The longer wavelength band has a red shift with a larger number of molecules. The band at 320 nm is the band of π -electrons of the benzene ring. By its nature, the maximum at 350 nm is characterized by the transfer of π -electrons from the benzene ring to the barbituric acid ring (intramolecular transfer). A band having a red shift is observed during aggregation and is a band with charge transfer from one molecule to another (intermolecular transfer).

Conclusion

The unusual fluorescence of DM was investigated theoretically by the DFT method and its time-dependent variant TDDFT.

Calculations carried out using Zindo, as well as *ab initio* calculations, confirm the appearance of a new band during aggregation and its shift to the red region when the number of molecules increases.

According to the calculated data, when aggregation of a large number of DM molecules, the absorption band of a monomolecule splits into several, and at the same time, a charge transfer band appears, which shifts to a longer wavelength region as the number of molecules increases.

The obtained theoretical calculations are consistent with experimental data [12]. According to experimental data, the maximum absorption and fluorescence of DM in the solid state compared to solutions is shifted to a longer wavelength region. Moreover, the intensity of fluorescence of DM in the solid state is significantly higher than that of fluorescence in solution. This is due to the fact that many intermolecular hydrogen bonds are formed in the solid state, that is, aggregations are obtained.

Calculations confirm that the greater the number of molecules involved in aggregation, that is, the more hydrogen bonds between DM molecules, the more the absorption maximum shifts. Thus, our calculations confirm the fact that due to the formation of hydrogen bonds between molecules, the intensity of the absorption and fluorescence bands increases and a shift to the red region is observed.

References

- 1 He W., Zhang Z., Luo Y., Kwok R.T.K., Zhao Zh. & Tang B.Zh. (2022). Recent advances of aggregation-induced emission materials for fluorescence image-guided surgery. *Biomaterials*, 288, 121709. <https://doi.org/10.1016/j.biomaterials.2022.121709>
- 2 Chen L., Wang X., Yuan Y., Hu R., Chen Q., Zhu L., Gu M. & Shen Ch. (2022). Photosensitizers with aggregation-induced emission and their biomedical applications. *Engineered regeneration*, 3(1), 59-72. <https://doi.org/10.1016/j.engreg.2022.01.005>
- 3 Sa Sh., Sahoo A., Mukherjee S., Perumal A. & Venkatasubbaiah K. (2022). N-C chelated tetraaryl-pyrazole based organoboranes: A new class of aggregation induced enhanced emission materials. *Dyes and Pigments*, 206, 110585. <https://doi.org/10.1016/j.dyepig.2022.110585>
- 4 Yin Y., Hu H., Chen Zh., Liu H., Fan C. & Pu Sh. (2021). Tetraphenylethene or triphenylethylene-based luminophors: Tunable aggregation-induced emission (AIE), solid-state fluorescence and mechanofluorochromic characteristics. *Dyes and Pigments*, 184, 108828. <https://doi.org/10.1016/j.dyepig.2020.108828>
- 5 Yu Q., Chen Sh., Han Ch., Guo H. & Yang F. (2020). High solid fluorescence of novel tetraphenylethene-porphyrin. *Journal of Luminescence*, 220, 117017. <https://doi.org/10.1016/j.jlumin.2019.117017>
- 6 Liu Y., Tang Yh., Barashkov N.N., Irgibaeva I.S., Lam J.W.Y., Hu R., Birimzhanova D., Yu Y. & Tang B.Zh. (2010). Fluorescent chemosensor for detection and quantitation of carbon dioxide gas. *J. Am. Chem. Soc.*, 132(40), 13951-13953. <https://doi.org/10.1021/ja103947j>
- 7 Shafiq N., Arshad U., Zarren G., Parveen Sh., Javed I. & Ashraf A. (2020). A comprehensive review: bio-potential of barbituric acid and its analogues. *Current organic chemistry*, 24(2), 129-161. <https://doi.org/10.2174/1385272824666200110094457>
- 8 Zhang H., Tian Y., Tao F., Yu W., You K., Zhou L-R., Su X., Li T. & Cui Y. (2019). Detection of nitroaromatics based on aggregation induced emission of barbituric acid derivatives. *Biomolecular Spectroscopy*, 222, 117168. <https://doi.org/10.1016/j.saa.2019.117168>
- 9 Shi W., Zhao S., Su Y., Hui Y. & Xie Z. (2016). Barbituric acid-triphenylamine adduct as an AIEE-type molecule and optical probe for mercury (II). *New J. Chem.*, 40(9), 7814-7820. <https://doi.org/10.1039/C6NJ00894A>.
- 10 Gaussian 98, Revision A3. Gaussian, Inc., Pittsburgh, PA, 1998.
- 11 Casida M.E. (1995). Recent Advances in Density Functional Methods, Part I, World Scientific, Singapore.
- 12 Mendigalieva S.S., Birimzhanova D.A., Irgibaeva I.S., Barashkov N.N. & Sakhno Y.E. (2022). Aggregation-induced emission of 5-(benzylidene)pyrimidine-2,4,6-triones. Bulletin of the Karaganda University. *Chemistry Series*, 105(1), 39-49. <https://doi.org/10.31489/2022Ch1/39-49>.

Information about authors*

Birimzhanova, Dinara Asylbekovna — PhD on Chemical Sciences, Senior lector, L.N. Gumilyov Eurasian National University, Satpayev street, 2, 010000, Astana, Kazakhstan; e-mail: dinarabirimzhanova@gmail.com; <https://orcid.org/0000-0002-5572-9339>

Irgibaeva, Irina Smailovna (*corresponding author*) — Doctor of Chemical Sciences, Professor of Chemistry Department, L.N. Gumilyov Eurasian National University, Satpayev street, 2, 010000, Astana, Kazakhstan; e-mail: irgsm@mail.ru; <https://orcid.org/0000-0003-2408-8935>

Barashkov, Nikolay Nikolayevich — Doctor of Chemical Sciences, Director of R&D and Technical Services Micro-Tracers, Inc. 1370 Van Dyke Avenue San Francisco, CA 94124, USA; e-mail: nikolay@microtracers.com; <https://orcid.org/0000-0003-2494-9248>

*The author's name is presented in the order: *Last Name, First and Middle Names*